Squares that look round: transforming spherical images

Saul Schleimer
Mathematics Institute
University of Warwick

Henry Segerman
Department of Mathematics
Oklahoma State University

Abstract

We propose Möbius transformations as the natural rotation and scaling tools to use when editing spherical images. As applications we show how to obtain Droste and other interesting visual effects using Möbius, and other conformal transformations.

1 Introduction

Interest in spherical imagery has grown in recent years, driven by increased accessibility of both viewing devices and cameras. The YouTube application on smartphones now plays spherical video, using the phone's accelerometer. Many virtual reality headsets are expected to be released in the near future. On the camera side, numerous consumer-focused spherical cameras are available, as well as high-end professional offerings.

Almost universally, spherical images and video are stored and transmitted via *equirectangular projection*: points on the sphere are given by their latitude and longitude. Thus the whole image is stored as a rectangular image with a two-to-one aspect ratio, corresponding to angles $(0, 2\pi) \times (-\pi/2, \pi/2)$. This data format fits conveniently into the infrastructure already in-place for ordinary images. However, there is a problem in editing spherical images; software developed for ordinary rectangular images does not know about the equirectangular projection. For example, one cannot rotate a spherical image about an axis other than the vertical axis using standard rectangular editing tools.

Future editing tools for spherical images will no doubt include the ability to rotate images around any axis, giving analogues of both translation and rotation of flat images. However, we can also ask what zooming might mean for spherical images, and what other transformations would be useful in spherical image editing. In the next section, we discuss *Möbius transformations*. These include ordinary rotations of the sphere, natural zoom-like transformations, and other interesting effects. In the sections after, we explore visual effects derived from other conformal transformations of the sphere.

Acknowledgements: The second author was inspired to investigate the action of Möbius transformations on spherical images by a paper of Sébastien Pérez-Duarte and David Swart [6]. He began work whilst visiting *eleVR* (a research group consisting of Emily Eifler, Vi Hart and Andrea Hawksley) and wrote a guest blog post[1] explaining the implementation of Möbius transformations. The Python code used to generate many of these images is available at *GitHub*[2].

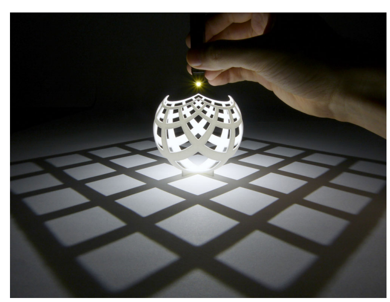

Figure 1: Stereographic projection from the sphere to the plane.

2 Möbius transformations

Möbius transformations act on the *Riemann sphere*, $\widehat{\mathbb{C}} = \mathbb{C} \cup \{\infty\}$. This is the result of adding a single point, ∞, to the complex plane $\mathbb{C}$. We map from the unit sphere S^2 in $\mathbb{R}^3$ to the Riemann sphere using stereographic

[1] http://elevr.com/spherical-video-editing-effects-with-mobius-transformations/

[2] https://github.com/henryseg/spherical_image_editing

projection [5, page 57]:

$$\rho(u,v,w) = \frac{u+iv}{1-w}$$

We set $\rho(0,0,1) = \infty$. Every other point of the unit sphere maps to a point of $\mathbb{C}$. Figure 1 shows a 3D printed visualisation of stereographic projection.

The *Möbius transformation* $M = (a,b;c,d)$ is the map from the Riemann sphere to itself given by

$$M(z) = \frac{az+b}{cz+d}, \quad \text{where } a,b,c,d \in \mathbb{C} \text{ and } ad-bc \neq 0.$$

There are various special cases involving the point at infinity. If $cz+d = 0$ then $M(z) = \infty$. If $c \neq 0$ then $M(\infty) = a/c$. If $c = 0$ then $M(\infty) = \infty$. There is a cleaner definition, avoiding these special cases, which uses the one-dimensional complex projective space, $\mathbb{CP}^1$. However, here we will stick with $\widehat{\mathbb{C}}$.

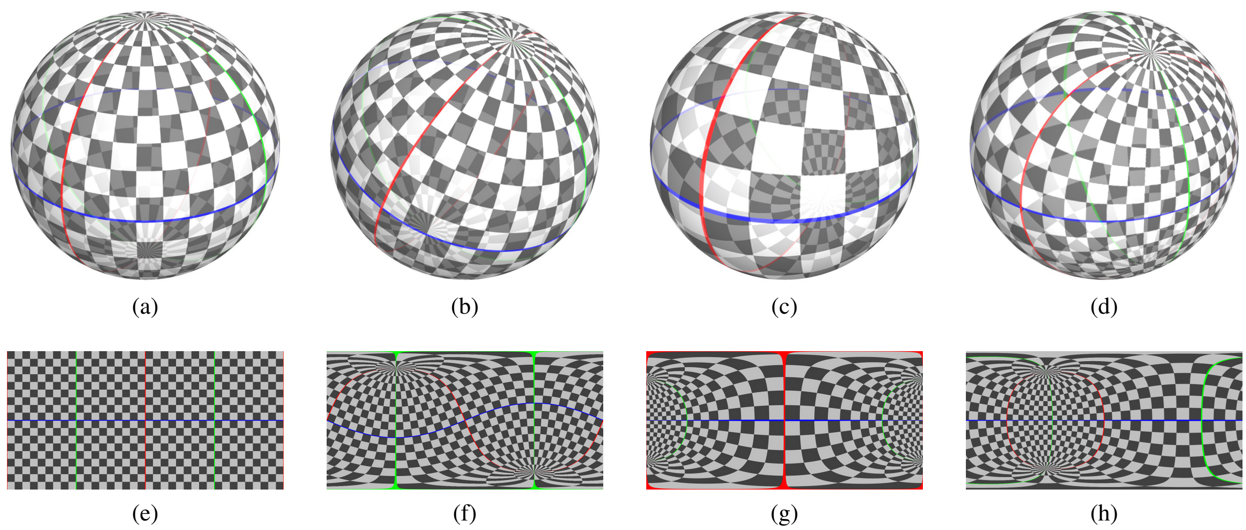

Figure 2: A test pattern (a and e), and the results of rotating by $\pi/8$ (b and f), scaling by a factor of two (c and g) and applying the parabolic translation $M(z) = z+1/2$ (d and h). Above: the textures on the sphere. Below: their equirectangular projections. Note that we generally view a spherical photograph from inside the sphere. From this perspective the equirectangular projections have the same orientation as the textures on the spheres.

We can rotate the complex plane about 0 by multiplying by a unit complex number, say $e^{i\theta}$. We can scale the plane, again centered on 0, by multiplying by a real number, say $\lambda \in \mathbb{R}$. Finally, we can translate the plane by adding a complex number, say w. These give the Möbius transformations $M = (e^{i\theta},0;0,1)$, $M = (\lambda,0;0,1)$, and $M = (1,w;0,1)$, respectively. These three kinds of transformations, called *elliptic*, *hyperbolic*, and *parabolic* respectively, are in some sense universal.

Figure 2 (top row) shows an initial test pattern, and the results of applying a rotation by $\theta = \pi/8$, of scaling by a factor of $\lambda = 2$, and of adding $w = 1/2$. The parabolic case is included for completeness; it is not clear how this might be used in image editing. Here we have placed zero, the origin of the complex plane, at the "front pole" of the sphere: the front intersection of the blue equator and red longitude. Note how the hyperbolic transformation scales up distance by a factor of two at zero but scales *down* by a factor of two at the antipodal point, ∞. In fact, Möbius transformations allow us to rotate or scale fixing any two points of the sphere. As an example, see Figure 3; we show a frame of raw footage and the transformed frame from a video[3] exploring many of the effects in this paper.

[3] https://www.youtube.com/watch?v=oVwmF_vrZh0

Every Möbius transformation distorts spherical distances to a greater or lesser degree; however in every case the right angles of the test pattern always remain right angles. Möbius transformations are *conformal*: they preserve all angles. Thus images are not sheared or non-uniformly stretched; features remain essentially recognisable. All of the transformations in this paper mapping the sphere to itself are conformal, apart from at a discrete set of points. Note that the equirectangular projection is not conformal; both distances and angles are distorted.

(a) The input image.

(b) The result of rotating by an angle of $\pi/12$.

Figure 3: Rotating a spherical photograph of Vi Hart and Henry Segerman, about Vi's eyes.

3 Other transformations

If we want to apply a "forward transformation" T to a pixel-based input image, we need to find the inverse transformation $S = T^{-1}$. This is because the algorithm to generate the output image from the input runs in reverse: for each pixel p of the output, we take its position z, compute $S(z)$, and assign p the same color as that at position $S(z)$ of the input. (In fact we take a weighted average of colors of input pixels nearest to $S(z)$.) We call this procedure *pulling back* via S or, equivalently, *applying* T. Thus the transformation $S = T^{-1}$ must be single-valued, but T need not be.

For Figure 4b we used $T(z) = \pm\sqrt{z}$ and $S(z) = z^2$; the resulting image is a "branched double-cover" of the room shown in Figure 4a. There is a new feature in this image, the *branch points*, around which nearby imagery is repeated. The number of repetitions is the *order* of a branch point. Here the branch points, of order two, are at zero and infinity and thus are on the floor and the ceiling; Figure 4c shows the spherical image in Figure 4b, rotated to show the branch point at zero in the center. These new features, the branch points, are unavoidable: any conformal transformation of $\widehat{\mathbb{C}}$ either has branch points or is a Möbius transformation [1, Section 4.3.2].

Figure 4d shows the result of pulling back via a variant of the complex exponential map, specifically $S(z) = -e^{-\lambda\left(\frac{1+z}{1-z}\right)}$. Here λ is a scaling parameter and the Möbius transformation $M(z) = \frac{1+z}{1-z}$ is a rotation by $\pi/2$ about $\pm i$; this ensures that the image repeats horizontally rather than vertically. In this case, the forward transformation $T(z)$ is a variant of the complex logarithm, so is infinitely valued. Thus the output contains infinitely many copies of the input image. The branch points are again on the floor and the ceiling, but are of infinite order.

The same techniques can be used to combine different spherical images into a single spherical image. This provides a spherical analogue of the familiar "split screen" trope in rectangular video: compositing multiple video clips into a single screen. We, however, can stitch the different images seamlessly, if they match along suitable arcs between the branch points. We created a spherical video along these lines, in which the second author appears to be in a two-fold branched cover of his apartment[4]. The footage is

[4] `http://www.youtube.com/watch?v=UUW_ZU3_TQM`

(a) The input image.

(b) Pulling back by $S(z) = z^2$.

(c) Figure 4b, rotated to show an order two branch point at the center.

(d) Pulling back via $S(z) = -e^{-4\left(\frac{1+z}{1-z}\right)}$.

Figure 4: Transformations applied to a spherical photograph featuring Emily Eifler, Vi Hart, Andrea Hawksley, and Henry Segerman, all shown twice. In these images the origin $0 \in \mathbb{C}$ corresponds to the top of the equirectangular projection while infinity corresponds to the bottom, other than for Figure 4c.

stitched together with a video of the empty apartment, so that only one copy of the author appears in the combined video.

4 The Droste effect

A common artistic and mathematical motif is that of "self-similarity"; this is often called the *Droste effect* in commercial and computer graphics. A "straight Droste effect", as found on the packaging of the eponymous Dutch cocoa, is obtained when the entire picture is included, under a shrinking transformation, inside of itself. The "twisted Droste effect" was first introduced by M.C. Escher in his *Print Gallery* lithograph. The mathematics behind Escher's image was explained by Bart de Smit and Hendrik Lenstra [2].

It is possible to obtain both the straight and twisted Droste effect in spherical images using Möbius transformations, the complex exponential map, and the complex logarithm (see also [6, page 223]). We simplify the discussion here by suppressing all mention of equirectangular and stereographic projections. We begin with a spherical image, say Figure 4a. We remove everything inside a small disk (here the inside of the frame on the wall) and everything outside a larger disk, to obtain a *Droste annulus*; see Figure 5a. We arrange matters so that there is a scaling transformation $M(z) = \lambda z$ that takes the outer boundary of the annulus to the inner boundary. Thus we may tile the sphere (minus two points) by copies of the annulus, obtaining a straight Droste image; see Figure 5b.

If we apply the logarithm to the Droste annulus then the annulus unwraps to give an infinite vertical strip in $\mathbb{C}$ with width $\log \lambda$; see Figure 5c. Another way to now obtain the straight Droste effect is to tile the plane by horizontal translations of the strip and apply the exponential map. Following De Smit and Lenstra [2, Figure 10], we may instead scale and rotate so that the rectangle shown in Figure 5d is vertical and has

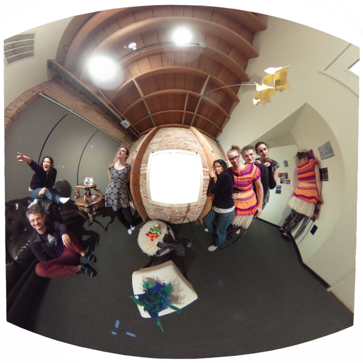

(a) A Droste annulus.

(b) A straight Droste image.

(c) Log Droste annulus.

(d) A different fundamental rectangle.

(e) A twisted Droste image.

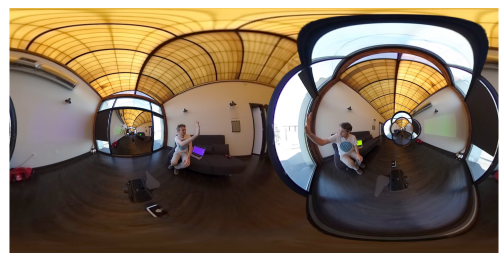

(f) Different images can be used for different zooms.

Figure 5: Droste effect images. These images answer the question of what it looks like from the inside of a Droste effect image: there is a flower-shaped portal floating in the middle of the room.

height 2π. Applying the exponential map yields Figure 5e.

Figure 5f shows a still image from a straight Droste video[5] in which the translated images are also offset in time. The duration of the time offset matches the flight time of the camera; thus the video loops.

All constructions of Droste effect images seem to involve "cut-and-paste" techniques; here we had the choice of frame and the choice of scaling. In contrast, the pull-back techniques of Section 3 can be applied to any spherical image whatsoever. The output is seamless; the only blemishes are the branch points.

5 Weierstrass and Schwarz-Christoffel

The complex exponential and logarithm are just two of the many beautiful flowers in the field of complex analysis. More exotic "elliptic" or even "modular" functions will give interesting visual effects when applied to spherical images. Here we will restrict ourselves to the Weierstrass $\wp$–function for the square lattice; we refer to [1, Chapter 7] for an excellent and short introduction. As a series the function is:

$$\wp(z) = \frac{1}{z^2} + \sum \left(\frac{1}{(z-\omega)^2} - \frac{1}{\omega^2} \right).$$

[5] `https://www.youtube.com/watch?v=qvh-EAipIUk`

(a) The two-fold branched covering maps from the torus to the sphere by "folding" the torus around the red "skewer". The four skewered points of the torus become the four red dots on the sphere.

(b) Cutting open the torus yields a square.

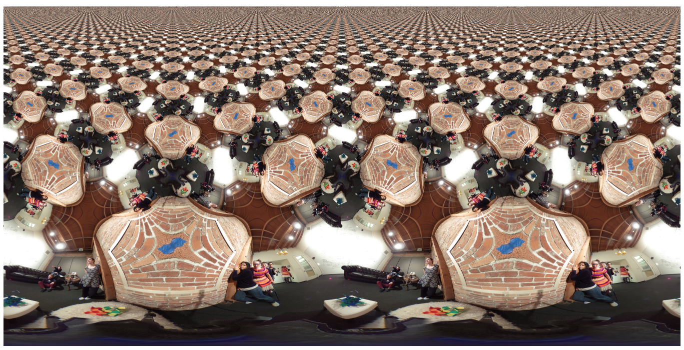

(c) The square tiles the complex plane; here viewed after applying inverse stereographic and equirectangular projection maps.

(d) Pull back the tiling in $\mathbb{C}$ via the map $z \mapsto (1+i) \cdot z$.

(e) Map down to the sphere again via Schwarz-Christoffel.

(f) The result if we pull back by $z \mapsto 2 \cdot z$.

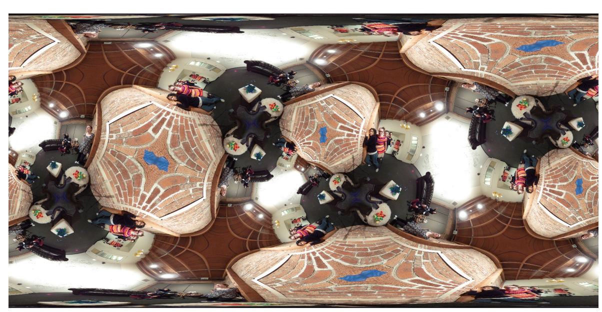

(g) The result if we pull back by $z \mapsto (2+i) \cdot z$.

(h) The result if we pull back by $z \mapsto (3+i) \cdot z$.

Figure 6: Images produced using Weierstrass and Schwarz-Christoffel maps.

The sum ranges over the non-zero Gaussian integers $\omega \in \mathbb{Z}[i]$. It is a non-trivial exercise to check that $\wp(z+1) = \wp(z+i) = \wp(z)$. So the Weierstrass function is *doubly periodic* – the exponential function is only singly periodic: $\exp(z+2\pi i) = \exp(z)$. The above series development for $\wp$ converges too slowly to be computationally useful. A version of $\wp$ using theta-functions should instead be used [4, page 132].

Since $\wp$ is doubly periodic, we can think of it as first mapping the plane $\mathbb{C}$ to the square torus $\mathbb{T}$, which then maps to the Riemann sphere $\widehat{\mathbb{C}}$ via a branched double-cover. So, we start with our standard spherical image (Figure 6a, left). We pull back to $\mathbb{T}$ and obtain a toroidal image (Figure 6a, right). Note that the toroidal image contains two copies of the original, and has four branch points. Cutting $\mathbb{T}$ open we obtain Figure 6b; a square containing two copies of the original, spherical, image. This is the unit cell of a tiling of $\mathbb{C}$, obtained by pulling back via $\wp$. This is shown in equirectangular form in Figure 6c.

Just as the exponential function has its logarithm, the Weierstrass $\wp$–function has a conformal inverse, which we denote by $\mathfrak{sc}_4$. For reasons of symmetry the inverse $\mathfrak{sc}_4$ is a map from the disk to the square. This, then, is a *Schwarz-Christoffel* function [1, Section 6.2.2]. In general, these functions are given by difficult integrals, but for regular n–gons there is a very pretty expression in terms of the hypergeometric function [3, Exercise 5.19]:

$$\mathfrak{sc}_n(z) = z \cdot {}_2F_1\left(\frac{2}{n}, \frac{1}{n}; 1 + \frac{1}{n}; z^n\right).$$

We are now ready to "twist", in similar spirit to the twisted Droste effect. We pull back the tiling in $\mathbb{C}$ via the map $z \mapsto (1+i) \cdot z$. A unit cell for this finer tiling is shown in Figure 6d. We pull this back to $\widehat{\mathbb{C}}$ using the map $\mathfrak{sc}_4$ and obtain Figure 6e. Since the overall map from $\widehat{\mathbb{C}}$ to $\widehat{\mathbb{C}}$ is conformal, apart from at a finite set of points, it is in fact *rational* [1, Section 4.3.2]: in this case it is the function $f(z) = \frac{i}{2}(-z + 1/z)$. Pulling back (in $\mathbb{C}$) by other Gaussian integers gives other interesting effects; see Figures 6f, 6g, and 6h.

6 Schottky groups

Suppose that a and b are hyperbolic (that is, zoom-like) Möbius transformations. Suppose that D_a, D_A, D_b, D_B are four closed disjoint disks in $\widehat{\mathbb{C}}$ so that a maps the interior of D_A onto the exterior of D_a, and similarly for b. Then the group generated by a and b is called a two-generator *Schottky group* [5, page 98].

Schottky groups can be used to generate impressive images; for a richly illustrated introduction to the underlying mathematics please see [5]. David Gu has also experimented with applying Schottky reflection groups to photographs[6]. We now discuss how to apply these ideas to spherical images.

We begin with an input image Figure 7a. We must choose the positions of the disks D_a, D_A, D_b, and D_A. In the final image these will contain zoomed copies of (part of) the input image. For D_a we choose the window; for D_b we choose the large round mirror lying below the camera, on which the tripod is standing. We trace over D_a and D_b in Photoshop to make a mask image in which the window is red and the mirror green, as shown in Figure 7b. We now choose two hyperbolic Möbius transformations, A and B, and set $D_A = A(\widehat{\mathbb{C}} - D_a)$, in white, and $D_B = B(\widehat{\mathbb{C}} - D_b)$, in blue. We choose A and B so that the all of the disks are disjoint, and no disk covers an important part of the input image. Let $a = A^{-1}$ and define b similarly.

To generate the image[7] shown in Figure 7c, for each pixel p, we perform the following routine.

1. Set $q = p$.
2. If q lies in the black region of the mask, color p the same as the color of q and stop the routine.
3. If q lies in D_X then replace q by $x(q)$ and go to step 2.

In general, a Schottky group can have taken more than two generators, or indeed fewer. Using just one generator recovers the straight Droste effect; $\widehat{\mathbb{C}} - (D_a \cup D_A)$ is the Droste annulus.

[6] See `http://www3.cs.stonybrook.edu/~gu/lectures/lecture_1_Escher_Droste_Effect.pdf`.

[7] Also see an animated version: `https://www.youtube.com/watch?v=vtWtmTzGxd4`.

(a) The input image.

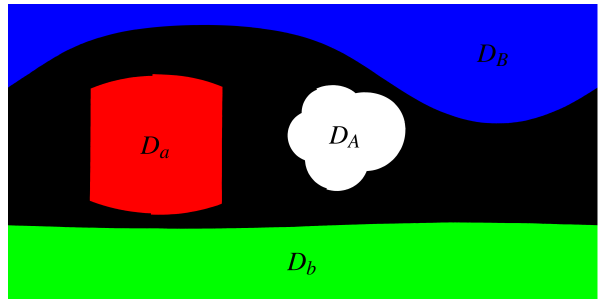

(b) The disks D_a, D_A, D_b, D_B in the Riemann sphere.

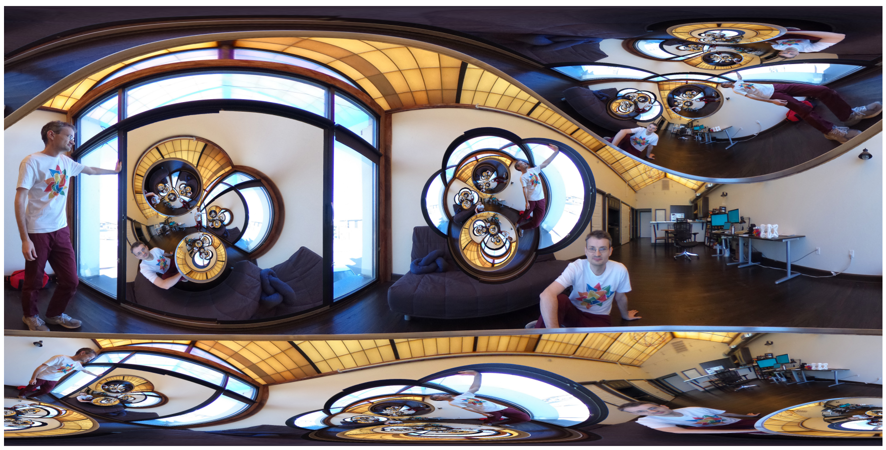

(c) A spherical Schottky image.

Figure 7: A spherical double Droste effect, using a Schottky group.

It is interesting to ponder how one might apply the twisted Droste effect throughout a Schottky image, but that is a task for another day.

References

[1] Lars V. Ahlfors. *Complex analysis: An introduction of the theory of analytic functions of one complex variable*. Second edition. McGraw-Hill Book Co., New York-Toronto-London, 1966.

[2] Bart de Smit and Hendrik W. Lenstra Jr. The mathematical structure of Escher's Print Gallery. *Journal of the American Mathematical Society*, 50(4):446–451, 2003.

[3] Jane M. McDougall, Lisbeth E. Schaubroeck, and James S. Rolf. Mappings to polygonal domains. In *Explorations in complex analysis*, Classr. Res. Mater. Ser., pages 271–315. Math. Assoc. America, Washington, DC, 2012.

[4] Henry McKean and Victor Moll. *Elliptic curves*. Cambridge University Press, Cambridge, 1997. Function theory, geometry, arithmetic.

[5] David Mumford, Caroline Series, and David Wright. *Indra's pearls*. Cambridge University Press, New York, 2002. The vision of Felix Klein.

[6] Sébastien Pérez-Duarte and David Swart. The Mercator redemption. In *Proceedings of Bridges 2013: Mathematics, Music, Art, Architecture, Culture*, pages 217–224. Tessellations Publishing, 2013. Available online at `http://archive.bridgesmathart.org/2013/bridges2013-217.html`.